Four-Dimensional Modeling of Two Ternary Columnar Composite Compounds

Hanna Karlsson

Master Thesis in Materials Chemistry, 2015
Department of Polymer and Materials Chemistry
Lund University
Sweden

Four-Dimensional Modeling of Two Ternary Columnar Composite Compounds

by

Hanna Karlsson

LUND
UNIVERSITY

Department of Polymer and Materials Chemistry
June 2015

Supervisor: **Professor Sven Lidin**
Examiner: **Professor Jan-Olle Malm**

Postal address
P.O. Box 124
SE-221 00 Lund, Sweden
Web address
www.polymat.lth.se

Visiting address
Getingevägen 60

Telephone
+46 46-222 00 00

Telefax
+46 46-222 40 12

Preface

This report is issued as a compulsory task of a master degree project in materials chemistry at the technical department of Lund University (LTH). The project was carried out at the department of polymer and material chemistry, it covered 30 ECTS and proceeded during the spring 2015.

The greatest thanks goes to my supervisor Sven Lidin who, despite his already extremely busy calendar, managed to squeeze in many long meetings and discussions. This project have been truly inspiring and not to mention very complicated from time to time. Mostly inspiring though, thanks!

I would also like to thank all the PhD students at the department and Gunnel Karlsson who helped me with the instructions of apparatus and techniques. I know you had a lot to do, thank you for your time and knowledge!

A special thanks goes out to Alfred Carlsson who, just as I, struggled to understand higher dimensions. Thanks for the many intensive conversations, my project would not have been as fun without you!

Over and out,

H.K

Lund, Sweden
June 2015

Abstract

Two ternary columnar composite crystals, $Ba_{15}Zr_{14}Se_{42}$ and $Sr_{21}Ti_{19}Se_{57}$, have been characterized and modeled three-dimensionally [1] and they are stated to have a commensurate crystal structure similar to several incommensurate ternary sulfur compounds [2]–[6]. To evaluate whether the two columnar compounds are isostructural to the sulfur compounds they need to be modelled four-dimensionally.

Four-dimensional models of $Ba_{15}Zr_{14}Se_{42}$ and $Sr_{21}Ti_{19}Se_{57}$ were simulated from existing three-dimensional data. The structures crystalize in the four-dimensional superspace group R-3m(00γ)0s with trigonal symmetry. The lattice parameters for $Ba_{15}Zr_{14}Se_{42}$ are $a = b =$ 12.4366 Å, c = 3.2681 Å and a q-vector ($\alpha\beta\gamma$) where α=β=0, γ = 15/28. Harmonic functions were used to describe the occupancy of the barium and selenium atoms. The overall structure was refined down to a residual factor of *wR(obs)* = 4.98%. For $Sr_{21}Ti_{19}Se_{57}$ the lattice parameters are $a = b$ = 11.9517 Å, c = 3.1026 Å and a q-vector ($\alpha\beta\gamma$) where α=β=0, γ = 21/38. The model was refined down to *wR(obs)* = 4.67% and in the same way harmonic functions were used for the occupancy of strontium and selenium. Both the models were compared to a previously modelled structure $Sr_{9/8}TiSe_3$ and great similarities were found between the two systems, indicating that they are indeed isostructural.

During the synthesis a new compound $Ba_{21}Zr_{12}Se_{45}$ was identified. It differs from the above mentioned in its Ba-Zr ratio and does not form the same columnar composite structure. It crystallizes in the trigonal three-dimensional space group R-3m (no. 166) with cell parameters $a = b$ = 21.9115(19) Å and c = 16.7445(9) Å. It was refined down to a residual factor of *wR(obs)* = 7.60%.

Abstract (Swedish)

Två kommensurabla ternära föreningar, $Ba_{15}Zr_{14}Se_{42}$ och $Sr_{21}Ti_{19}Se_{57}$, har tidigare blivit karaktäriserade och modellerade i tre dimensioner [1] och har visat påtagliga likheter med flertalet inkommensurabla ternära svavelföreningar [2]–[6]. För att utvärdera om de olika föreningarna är isostrukturella måste en fyrdimensionell modell av de två kommensurabla föreningarna göras.

Fyrdimensionella modeller av $Ba_{15}Zr_{14}Se_{42}$ och $Sr_{21}Ti_{19}Se_{57}$ simulerades från redan befintlig tredimensionell data. Modellerna visade att strukturerna kristalliserar med trigonal symmetri i den fyrdimensionella rymdgruppen R-3m(00γ)0s. Gitterparametrarna som användes för $Ba_{15}Zr_{14}Se_{42}$ var $a = b$ = 12,4366 Å, c = 3,2681 Å med en q-vektor (αβγ) där α=β=0, γ = 15/28. Harmoniska funktioner användes för att beskriva okupansen av barium- och selenatomerna. Hela strukturen förfinades ner till en restfaktor på *wR(obs)* = 4.98%. För $Sr_{21}Ti_{19}Se_{57}$ var gitterparametrarna $a = b$ = 11.9517 Å, c = 3.1026 Å och en q-vector (αβγ) där α=β=0, γ = 21/38. Modellen förfinades ner till *wR(obs)* = 4.67% och på samma sätt användes harmoniska funktioner för att beskriva okupansen av strontium och selen. Modellerna jämfördes sedan med en tidigare modellerad struktur, $Sr_{9/8}TiSe_3$, och stora likheter kunde hittas vilket tyder på att föreningarna är isostrukturella.

Under syntetiseringen hittades en ny förening $Ba_{21}Zr_{12}Se_{45}$ som inte finns dokumenterad sedan tidigare. Den skiljer sig från ovannämnda förening i barium/zirkon-förhållandet. Den nya föreningen bildar inte samma långa kompositstruktur vilket resulterar i en betydligt mindre enhetscell. Strukturen förfinades tre-dimensionellt ner till en restfaktor på *wR(obs)* = 7,60 % Den visade sig kristallisera i rymdgruppen R-3m (nr. 166) men cellparaetrar $a = b$ = 21,9115(19) Å och c = 16,7445(9) Å.

Table of Contents

1. Introduction

A composite crystalline compound holds a structure that can be divided into at least two different subunits with their own lattice constants [7]. There are cases where these subunits order differently within the unit cell which can lead to unusually large unit cells [1]. If the compound is a so called chain-type composite this means that the subunits form chains, within the unit cell, that follow different repeat patterns. These type of compounds have been found in ternary sulfur systems including strontium-titanium [2]–[4], [6] and barium-titanium [5]. Due to their incommensurability four-dimensional models have been made for these structures.

Two ternary selenium compounds including strontium-titanium and barium-zirconium have been found and are thought to be commensurate cases with similar structures as the sulfur systems mentioned above [1]. Three-dimensional models have been made for the two compounds and they were both found to have a rhombohedral structure. There might however be a possibility for the selenium compounds to be isostructural to the sulfur cases and in order to evaluate this, a four-dimensional model needs to be made. In this report such a model will be made and the two selenium compounds will be compared to the sulfur-structures.

1.1 Aim

The aim of this report is to make a four-dimensional model of the structures of two columnar composite compounds, $Sr_{21}Ti_{19}Se_{57}$ and $Ba_{15}Zr_{14}Se_{42}$. The ternary compounds will be synthesized and characterized and the four-dimensional model will be used to compare them with previously studied ternary sulfur compounds [2]–[6].

1.2 Scope

This report is issued as one of the compulsory parts of a master degree project at Lund University. In this report a model will be made for two commensurate columnar composite compounds, $Sr_{21}Ti_{19}Se_{57}$ and $Ba_{15}Zr_{14}Se_{42}$, using a four-dimensional formalism. The models will be used to investigate whether these two compounds are isostructural to previously evaluated structures including sulfur instead of selenium; Sr_xTiS_3 (x = 1.05-1.22) and Ba_xTiS_3 (x = 1.00-1.05), synthesized and studied by different research groups [2]–[6]. The two compounds, $Sr_{21}Ti_{19}Se_{57}$ and $Ba_{15}Zr_{14}Se_{42}$, will be synthesized and characterized using single crystal diffraction.

The beginning of the report will give a brief introduction and background to the project. A theory part will follow with a description of the ternary systems and a brief description of the characterization methods used in this report. The overall research methodology will then be described followed by the experimental method, where the laboratory procedures will be presented. The results will then be presented and discussed followed by conclusions and future work.

1.3 Limitations

The main limitation is the time span during which this project is to be carried out. A total period of approximately 20 weeks is recommended for a master thesis. Availability of apparatus as well as availability of the supervisor are also limiting factors that might not affect the project as a whole but the weekly planning. Difficulties regarding the synthesis have also limited this project which will be discussed further in the report.

2. Theoretical Background

The following sections will give a brief introduction to the foundation on which the work in this report is built on. It will cover the binary systems of the components as well as the different characterizations techniques used for the evaluation of the system.

2.1 Summary on Crystal Structures

Crystalline lattices are built from lattice points with identical surroundings and there are seven types of three-dimensional lattice systems (Cubic, Tetragonal, Orthorhombic, Hexagonal, Trigonal, Monoclinic and Triclinic). These lattice systems can then be divided into five lattice types; primitive, body-centered, rhombohedral and two types of face-centered. All in all 14 combinations are possible and these are called the Bravais lattices. Each combination of these is determined by symmetry requirements. In total there are 32 so called point groups related to the different possible symmetry operations and if they are combined with the Bravais lattices, 230 space groups are possible for three-dimensional crystal structures. [8]

2.2 Reciprocal Lattice

In crystallography the terms reciprocal space and reciprocal lattice is used. The atomic structure is described in the direct lattice while the diffraction pattern is described in reciprocal space. The origin of this geometrical construction is Bragg's law, which is defined as follows.

$$2d \sin\theta = n\lambda \qquad (2.1)$$

Where d is the interplanar spacing, θ is the reflection angle, n is an integer and λ is the wavelength. From this correlation it is clear that a large distance d in the atomic structure (direct space) leads to a small angle θ (reciprocal space) so that the reflections from a large unit cell structure generates a dense pattern and the reflections from a small unit cell structure generates a sparse pattern.

The reciprocal lattice relates to the actual lattice as follows; the reciprocal of the vector a (a^r) is normal to the $b-c$ plane and in the same way b^r is normal to the $a-c$ plane and c^r to the $a-b$ plane [9]. The mathematical correlations are as follows:

$$a^r \cdot b = a^r \cdot c = b^r \cdot a = b^r \cdot c = c^r \cdot a = c^r \cdot b = 0 \qquad (2.2)$$

$$a^r \cdot a = b^r \cdot b = c^r \cdot c = 1 \qquad (2.3)$$

The latter relation fixes the modulus and sense of the reciprocals. The reciprocal of a face-centered lattice is a body-centered lattice and the other way around. The other structures are the reciprocal of themselves. [9]

2.3 Commensurate and Incommensurate Composite Structures

There are structural cases where a significant part of the atoms in a crystal can adapt a so called superstructure. The original lattice with high symmetry will be a substructure in the lower symmetry superstructure [9]. A superstructure can be present for a number of reasons such as the presence of another lattice (composite structure), periodic lattice distortions,

magnetic structures and such [10]. The structures studied in this report are so called chain-like composite structures where the subunits are repeated in chains with different periodicity.

In crystallography when doing x-ray diffraction the superstructure will appear as weaker spots in the diffractogram and the substructure will appear as bright spots. For the case of commensurate structures the spots that represent the superstructures will be positioned at simple fractions of the vectors of the reciprocal lattice of the substructure. Incommensurate structures, on the other hand, occurs when the position of the spots related to the superstructures are not located at simple fractions of the vectors. Incommensurable systems are often found in structures where two competing periodicities are present, as the ones discussed in this report. Due to the simple fraction positioning in the commensurate case these structures can be translated into three-dimensional indexing whereas the incommensurate structures always need a four-dimensional indexation. [9]

2.4 Four Dimensional Modeling

The commensurate and incommensurate composite crystals structures consists of subunits with different periodicities. Common for the cases covered in this report is that the subunits in one structure share the lattice parameters *a* and *b* while they have different *c*-axes (c_1 and c_2) [1]–[6], [8]. Because of this, a three-dimensional model is only possible when the different *c*-axes relate to each other as in the commensurate case. If they do not, in the incommensurate case, both *c*-axes needs to be included in the model and hence a four-dimensional model need to be made.

The *c*-axis can be interpreted as the wave length of a sinusoidal curve that describes the deviation of the position of the atoms in the substructure. The curve will look different for the different subunits and thus c_1 is not equal to c_2. They however relate to each other according to $c_1 = \gamma \cdot c_2$, where the value of γ is either a simple fraction as for the commensurate cases or not as for the incommensurate case. In a general case, the q-vector has components in all three reciprocal directions, q = (α β γ), in the cases studied in this work, the *q*-vector is of the form (0 0 γ). [7]

As described above the reciprocal lattice have the basic vectors a^r, b^r, c^r. The reflection intensities that can be indexed from these vectors are called the main reflections and are the ones corresponding to the subunits of the cell. The weaker reflections, the satellites, are the ones that correspond to the superstructure and these can only be indexed using the basic vectors in commensurate cases. For incommensurate cases an extra vector is needed, the *q*-vector, which leads to a four-dimensional indexing. The indexing will thus consist out of four parameters (*hklm*) where *m* is the parameter arising from the *q*-vector and is thus equal to 0 for the main reflections. [7]

When naming the four-dimensional lattice the three-dimensional Bravais lattice type for the first subunit are named first followed by the *q*-vector. The fractional components of the glide-translation for the *q*-vector is then stated using the symbols *0*, *s*, *t*, *q* and *h* corresponding to translations of 0, 1/2, 1/3, 1/4 and 1/6 respectively. [7]

2.5 The Ternary Sulfur Compounds

The first report of a compound within the strontium-titanium-sulfur system was the stoichiometric compound $SrTiS_3$. It was published in 1956 by Hahn and Mutschke [11] and its structure was studied using powder diffraction. It was reported to have a $BaNiO_3$-type of structure but it could not be indexed from the powder data.

Further studies of the Sr-Ti-S system was later made by Saeki and Onoda [6] and revealed crystals holding so called columnar composite structures with the composition Sr_xTiS_3 ($1.05 \leq x \leq 1.22$). The results from these powder diffraction studies shows incommensurate behavior of the crystals and is not consistent with the previously published suggestion of a $BaNiO_3$-type structure. The reflections from the powder diffraction were indexed in hexagonal setting and it was suggested that the change in Sr-content gives rise to a change in the subcell periodicity, thus an infinite number of structures are possible for the ternary compound. It was also stated that some of the specimen crystallized in commensurate structures and some as incommensurate structures. The composite crystal structure was modelled from the interactions between the subcells. [6]

A refinement of the structure of the columnar compound $Sr_{1.145}TiS_3$ has also been made by Saeki and Onoda [4]. The crystals showed to have an incommensurate structure where units of $[TiS_{6/2}]$ and Sr atoms are repeated along the *c*-axis. The $[TiS_{6/2}]$-units consist out of face-shared octahedra, with titanium atoms at the center and sulfur atoms at the corner positions (TiS_6), and titanium atoms with a triagonal prism coordination. The strontium atoms are then packed in columns in the space between the chains of octahedrons. In the same way, the structure of $Sr_{1.19}TiS_3$ were evaluated and were found to have a similar structure as the $Sr_{1.145}TiS_3$ but with a higher strontium content [3]. The same authors have studied the tertiary system of Ba_xTiS_3 ($1.00 \leq x \leq 1.05$). This was the third example of chain-like composite crystals reported [5]. Also in this case titanium and sulfur constituted face-sharing octahedral units that repeated along the *c*-axis with barium atoms in between.

Another group of researchers, Gourdon and Petricek, have also been looking at the Sr-Ti-S system [2]. They have studied the compound $Sr_{9/8}TiS_3$. Instead of using powder diffraction as made in the previous studies this group made their characterization using single crystal diffraction. Compared to powder diffraction, single crystal diffraction is a more reliable method when characterizing crystals with a composition range as the sulfur compounds. The sample might look homogenous but consists of many different crystals. A four-dimensional model was made and the structure showed a trigonal symmetry within the four-dimensional superspace group R-3m(00γ)0s. The sulfur atoms in the structure are aligned in six disjointed rods where two of them are symmetry independent. One of these was described in the model with an occupancy following a crenel function. The other was then introduced, also this with an occupancy following a crenel function, but which was dependent and limited by the first one.

In the same way another crenel function was introduced to describe the strontium positions. The structure of the compound was found to have a different structure compared to those described by Saeki and Onoda. The structure is still thought to consist out the chains of $[TiS_{6/2}]$-units and strontium atoms but there is a lack of the trigonal prisms that were reported to function as coordination spheres (together with the octahedra) for the titanium atom by Saeki and Onoda [4]. Instead something in between a trigonal prism and an octahedral is reported in this study. [2]

2.6 The Ternary Selenium Compounds

Previous studies have stated that two columnar composite compounds, $Sr_{21}Ti_{19}Se_{57}$ and $Ba_{15}Zr_{14}Se_{42}$, holds a commensurate structure similar to those stated by Saeki and Onoda for the sulfur compounds. The results are based on synthesis and characterization of single crystals using single crystal x-ray diffraction. Space group and cell parameters were determined and both were found to have a rhombohedral structure, see Table 2.1 for

specification [1]. Both crystal structures viewed along the c-axis are presented in Appendix A.

Table 2.1. Three-dimensional space group and cell parameters for the two columnar selenium compounds [1].

Compound	Space group	*a* [Å]	*c* [Å]
$Sr_{21}Ti_{19}Se_{57}$	R-3	11.9517(5)	117.90(4)
$Ba_{15}Zr_{14}Se_{42}$	R-3c	12.4366(1)	91.5069(6)

For the $Ba_{15}Zr_{14}Se_{42}$ case, chains of $[ZrSe_{6/2}]$-units and barium atoms are repeated and form the unit cell. The $[ZrSe_{6/2}]$-units are linked together by face sharing octahedra. The long *c*-axis is obtained due to a mismatching in the repeat of the units through distorted trigonal prisms at 45.75 and 30.5 Å. [1] From the three-dimensional structure it can be found that for every 28 repeat of the $[ZrSe_{6/2}]$-units there is a repeat of 15 barium atoms.

In the same way the unit cell of $Sr_{21}Ti_{19}Se_{57}$ is built from repeating units of $[TiSe_{6/2}]$ and strontium atoms. Almost identical mismatching through trigonal prisms is found for the $[TiSe_{6/2}]$-units in this structure. Due to different repeat of the $[TiSe_{6/2}]$-units, four mismatching points can be found which makes the *c*-axis for this unit cell even longer, as can be seen in Table 2.1. [1]

In Figure 2.1 the two selenium compounds are presented together with the sulfur compound $Sr_{9/8}TiS_3$. As can be seen there are significant similarities between the three unit cells and the mismatching of the selenium and sulfur atoms are easily detected.

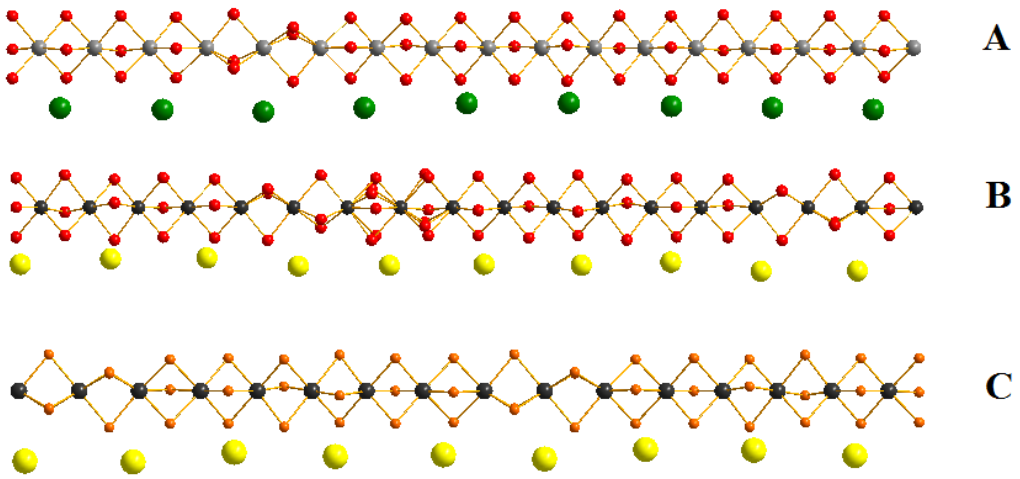

Figure 2.1. The unit cells of $Ba_{15}Zr_{14}Se_{42}$ (A), *$Sr_{21}Ti_{19}Se_{57}$ (B) and $Sr_{9/8}TiS_3$ (C) viewed along the a-axis. The atoms correspond to barium (green), selenium (red), strontium (yellow), sulfur (orange), titanium (dark grey) and zirconium (light grey). The mismatching in the repeat of selenium and sulfur atoms are apparent. The unit cells of $Ba_{15}Zr_{14}Se_{42}$ and $Sr_{21}Ti_{19}Se_{57}$ have been truncated to the same length as $Sr_{9/8}TiS_3$ for a better comparison.*

2.7 Characterization Methods

2.7.1 Single Crystal Diffraction

Single crystal diffraction is a characterization method used to determine the crystal structures and lattice parameters of one single crystal. X-rays of a known wavelength is directed towards the sample and scattered by the crystal lattice. If the scattered x-rays are in phase they fulfill Bragg's law and an intensity peak can be detected. If not, they are out of phase and cancel each other out, thus no intensity peaks appear [12].

The intensity and the Bragg angle is measured for each *hkl*-reflection. From the detected intensity peaks a pattern is obtained that function as a fingerprint for the crystal. [12]

2.7.2 Powder X-ray Diffraction

Powder x-ray diffraction is a characterization method used to determine crystal structures and lattice parameters for powders. The technique is similar to that of single crystal diffraction but instead of rotating one single crystal, reflections from randomly oriented crystals in the powder are being measured. Two different methods are possible, either transmission or reflection.[12]

3. Method

This report is issued as a compulsory part of a master thesis. It includes theoretical studies of the subject along with experimental work.

The work and results presented in this report is based on various methods of collecting information. A literature study and background theory were made using articles and literature obtained through scientific search engines. The data base "Pearson's Crystal Data" was used for obtaining known structures and other information that was useful.

The main parts of this project consisted of laboratory synthesis experiments. The synthesis was planned in collaboration with the supervisor. Instruction to the apparatus used was given by the supervisor and also occasionally by PhD students acquainted with the techniques. All the experiments were conducted at the department of materials and polymer chemistry, at Lund University, using the apparatus available.

Characterization was made using x-ray diffraction, mainly single crystal diffraction but powder diffraction was used to confirm the purity of intermediate components of the synthesis. The software WinXPOW was used to study the diffractograms obtained from the powder diffraction. For handling the raw data obtained from the single crystal diffraction the software CrysalisPro was used. The reflection data was integrated and exported as *hkl*-files. Superflip was used to solve the structure and JANA2006, together with Diamond 4.0, was used for the refinement of the parameters. The four-dimensional indexing was done using *hklm*-files obtained through Fortran based programs.

4. Experimental Method

All the handling of the starting materials were carried out in a glove box with argon atmosphere. This because of the water and air sensitivity of the chlorides and selenides. The synthesis of the two ternary compounds was performed according to previously conducted experiments [1]. No ampoule material was specified so different approaches were made in this study, they are presented in the following sections.

4.1 Synthesis of $Sr_{21}Ti_{19}Se_{57}$

The raw materials used for the synthesis were according to Table 4.1. The substances were mixed in a molar ratio of 1:1:2 for SrSe, Ti and Se. A flux of about 10 wt-% $SrCl_2$ was used for the synthesis. A more detailed description of each sample and the treatment it underwent can be found in Appendix B.

Table 4.1. Starting materials for the $Sr_{21}Ti_{19}Se_{57}$ synthesis.

Substance	CAS #	Purity [%]	Form	Supplier
SrSe	1315-07-7	99.99	Powder	Sigma Aldrich
Ti	7440-32-6	99.99	Granules	Alfa Aesar
Se	7782-49-2	99.99	Granules	KEBO
$SeCl_2$	14457-70-6	99.99	Powder	Sigma Aldrich

4.1.1 Synthesis in Quartz Tubes

The first attempt to synthesize the ternary Sr-Ti-Se compound was carried out in evacuated silica tubes. Starting materials were weighted in the glove box to an accuracy of 4 decimal places. The silica tubes were taken out of the glove box to be flushed with argon gas three times and evacuated down to 0 mbar before they were put in a chamber furnace. The samples were heated to 1050 °C which led to breakage of the silica tubes and the samples were lost. Another attempt was made where the samples were heated to lower temperatures (950 °C) to decrease the vapor pressure of selenium. This was also proven unsuccessful due to breakage of the quartz tube and oxidation of the sample. Thus, no synthesis could be performed in silica tubes.

4.1.2 Synthesis in Alumina Crucibles in Niobium Tubes

The next attempt to synthesize the samples was carried out in open alumina crucibles enclosed in evacuated niobium tubes. Samples was weighted in the glove box and put in an alumina crucible. The crucible was then enclosed in a niobium tube and removed from the box to be evacuated and sealed in an arc welder. The samples was flushed with argon three times and evacuated down to the limit of the vacuum system for the arc welder, 1 or 2 mbar. The niobium tubes were then put in Schlenk tubes which were flushed with argon two times and evacuated down to 0 mbar before they were put in a tube furnace. The furnace was heated to temperatures between 1000 and 1100 °C for different samples and the minimum annealing time was 80 h.

After the reaction and heat treatment the furnace was left to self-cool in most cases but an attempt was also made to lower the temperature more gradually over two days to study whether this made any changes to the samples.

This approach seemed more successful than the previous and the tubes were intact after the heat treatment. However, no needle-like crystals were found in the samples. It could be observed that the selenium had reacted with the niobium and formed a thin layer on the inside the tube. This could be the reason for the lack of crystals due to the loss, and thus wrong molar ratio, of selenium available for the wanted reaction.

4.1.3 Synthesis in Quartz Tubes Enclosed in Niobium tubes

Because of the volatility and thus loss of selenium due to the reaction with the niobium tube an attempt was made to make the synthesis in a quartz tube enclosed in a niobium tube. Water was added to the niobium tube to create a counter pressure that would help the quartz tube to stay intact. This was however proven unsuccessful since the quartz tube had exploded anyway and the sample was lost.

4.2 Synthesis of $Ba_{15}Zr_{14}Se_{42}$

The raw materials used for the synthesis were according to Table 4.2. The synthesis was carried out in two steps were BaSe was synthesized separately as a first step. Ba and Se were mixed in equimolar amounts for the binary synthesis and the ternary sample was then mixed in the molar ratios 1:1:2 for BaSe, Zr and Se. A flux of about 40 wt-% $BaCl_2$ was used for the ternary synthesis. A more detailed description of each sample and the treatment it underwent can be found in Appendix B.

Table 4.2. Starting materials for the $Ba_{15}Zr_{14}Se_{42}$ synthesis.

Substance	CAS #	Purity [%]	Form	Supplier
Ba	7440-39-3	N.A	Flakes	N.A
Se	7782-49-2	99.99	Granules	KEBO
Zr	7440-67-7	99.9	Slug	ABCR
$BaCl_2$	10361-37-2	99.999	Powder	Sigma Aldrich

4.2.1 Synthesis of BaSe

Binary BaSe was synthesized separately. First attempts were made to synthesize the compound in quartz tubes but it were proven unsuccessful and the quartz tubes broke during the reaction and the sample oxidized.

The BaSe could be synthesized in platinum tubes enclosed in evacuated stainless steel tubes. The elements were weighted in the glove box and then removed to be evacuated and sealed in the arc welder. The sample was flushed with argon three times and evacuated down to 1-2 mbar each time before put in a chamber furnace. The temperature was gradually increased and held at a temperature of 600 °C for 48 h. The temperature was then increased to 712 °C and held there for five hours before the oven was turned off and left to self-cool. The product was confirmed using powder XRD, presented in Appendix C.

4.2.2 Synthesis in Platinum tube in Niobium-tube

The ternary syntheses were made in a similar arrangement. The substances were weighted in the glove box and the synthesis were conducted in platinum tubes enclosed in evacuated niobium tubes, sealed and evacuated in the arc welder, flushed with argon three times and evacuated down to 1-2 mbar each turn. The samples were then annealed in evacuated Schlenk tubes at 1050 °C for different periods of time.

4.3 Characterization Methods

4.3.1 Single crystal diffraction

Preliminary single crystal diffraction was used to analyze the samples obtained from the synthesis. Single crystals were picked out from the sample and mounted on thin silica threads using epoxy glue.

The apparatus used was an Oxford Instruments device. Molybdenum was used as electron source with a wavelength of $\lambda = 0.7107$ Å and graphite was used as monochromator.

To analyze the raw data the software CrysAlisPro was used. The structures were then solved using Superflip and JANA2006 was used for the refinement.

4.3.2 Powder X-ray Diffraction

The apparatus used was a STOE Stadi Mp with vertical arrangement. It had a germanium monochromator and the X-rays came from a copper source (K α), $\lambda = 1.5418$ Å. The software used for the analysis was WinXPOW. The samples were grinded and put on an amorphous tape before the analysis.

4.4 Four-dimensional Modeling

From the known unit cells of the two ternary selenium compounds the repeat of the different subunits were found. An indexation of the two latter parameters in four-dimensions, *l* and *m*, was made by hand using these known repeats. The *l* parameter was indexed according to the repeat of the selenium-units (28 and 38 for the Ba-compound and Sr-compound respectively) and the *m* parameter to the repeat of the subunit consisting of the single atom chains (15 and 21 for Ba and Sr, respectively). *hkl*-reflections were then generated using a Fortran program and these were fitted and refined with the three-dimensional model to obtain a *hkl*-file that was consistent with the three-dimensional model.

The correlation between the main reflections and the satellites were then found from the handmade indexation. The correlations were written into a program that generates four-dimensional indexing (*hklm*) from the three-dimensional *hkl*-file. The *hklm*-file was then refined against a model in JANA2006.

5. Results and Discussion

5.1 Four-dimensional Modeling of $Ba_{15}Zr_{14}Se_{42}$

Random reflections were generated in Fortran, based on the size of the unit cell, to get a file with the right format to use as a base in JANA2006. This was then fitted to the crystal data obtained from the original article[1] so that the values in the *hkl*-file matched the actual structure.

The fitted *hkl*-file were then modified using another Fortran code. In this step the information about the structural factor were used to obtain information about the intensities for each *hkl*-reflection. The structural factor contains information about atomic positions and the scattering factor, and its square is proportional to the intensity of the reflections. The file now contains information about the *hkl*-reflections and their intensity, along with values of the standard deviation (σ).

An indexation of the *l* and *m* parameters were made by hand from the known repeat the different subunits in the unit cell. The repeats of the [ZrSe6]-units were found to be 28 and for the Ba-atoms it was found to be 15. The satellites (*m*) were indexed based on the main reflections (*l*) around a set reference (00). A table of the handmade indexation is presented in Appendix D.

The correlations between the parameters were found and written into a Fortran code to generate the four-dimensional parameters based on the three-dimensional reflection data. The latter *hkl*-file from the three-dimensional case were used and the *m*-parameter generated based on the value of *l*.

The *hlkm*-file that were the result of the four-dimensional re-indexing were imported and refined in JANA2006. The four-dimensional crystal parameters used are summarized in Table 5.1. The super space group were obtained by using superflip and agrees with that of the sulfur compounds, R-3m(00γ)0s.

Table 5.1. Crystallographic data for $Ba_{15}Zr_{14}Se_{42}$.

Crystal system	Trigonal
Space group	R-3m(00γ)0s
a* = *b	12.4366 Å
c	3.2681 Å
α = β	90 °
γ	120 °

When calculating the *hklm*-parameters from the three-dimensional data, all possible reflections for the structure are obtained. Since the reflection data is randomly obtained, the intensities might not be accurate compared to what a real data set would look like. This could result in the appearance and higher intensities of high order satellites that would not normally be present. Thus a poor fit for such reflections would increase the overall residual factor (R-value). More reflections locks the atoms to certain positions in the lattice that might not be totally accurate. Thus, if the amount of reflections could be lowered it might be possible to get more refined model. This was overcome by restrictions in JANA2006 that excluded satellites reflections higher than the order of five from the model.

The model was refined down to a R-value of 2.04% and 2.74% for the main reflections and the first order satellites respectively, with a goodness of fit (GoF) of 1.06. This is presented in Table 5.2 together with the R-values for the higher order satellites, the two subunits and the entire structure. The residual factor for the structure has a slightly higher value of 4.98% due to the contribution of the satellites.

Table 5.2. Final residual factors for the four-dimensional model of $Ba_{15}Zr_{14}Se_{42}$.

	R(obs) [%]	**wR(obs) [%]**	**Observed reflections/All**
Main reflections	1.87	2.04	482/703
1 order satellites	2.45	2.74	716/1090
2 order satellites	3.75	4.40	366/576
3 order satellites	6.45	8.15	163/386
4 order satellites	7.69	9.26	82/245
Structure	3.62	4.98	1979/3854
Sub1 [Ba]	2.04	2.22	158/256
Sub2 [$ZrSe_{6/2}$]	1.89	2.07	281/397
Common	1.36	1.55	43/50

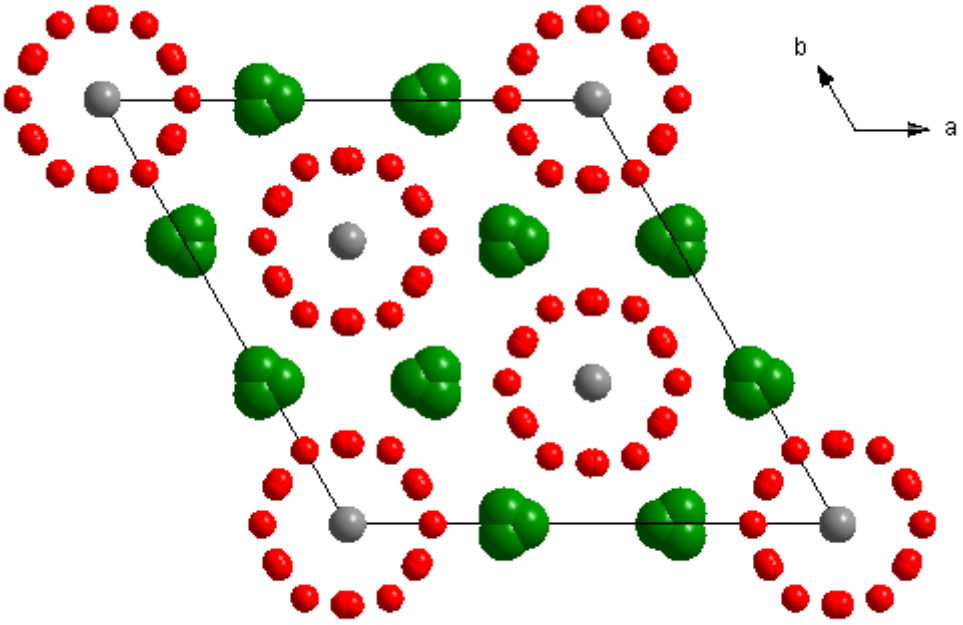

Figure 5.1. The structure obtained for $Ba_{15}Zr_{14}Se_{42}$ (viewed along the c-axis) from just translating the three-dimensional data into a four-dimensional model. This was the starting point of the refinement of the model. Atoms correspond to barium (green), selenium (red) and zirconium (light grey).

From Figure 5.1 it can easily be seen that from just translating the three-dimensional structure into four-dimensions the atoms holds approximately the correct position in the lattice. The big issue with this initial un-refined model is that more than one atom are holding

the position of one lattice point which of course is strictly forbidden and incorrect. Also, the selenium atoms do not cover all the positions they should.

For the barium position it is easy to see, when you compare it to the original structure obtained from data [1], that for each lattice position only one of the three atom positions should be present. In the original structure the barium atoms interact with $[ZrSe_{6/2}]$-units and are distorted along *c*-axis by moving from the three different sights seen in Figure 5.1. This is consistent with the model made for $Sr_{9/8}TiS_3$ where the modelling problem was solved using a crenel function for the occupancy of the Sr-atoms [2]. In this model harmonic functions were however used for the occupancy because they are easier to construct.

The same goes for the selenium atoms. In the work done by Gourdon et.al [2], the occupancy of two independent sulfur atoms were modeled using crenel functions. This is also applicable for our model but instead of crenel functions harmonic functions were used in this case as well. Two selenium atoms which occupancy are described by harmonic functions were defined. From the symmetry correlations the rest of the positions were obtained, also this consistent with $Sr_{9/8}TiS_3$ [2]. A comparison of the three-dimensional model, the four-dimensional model made in this study and $Sr_{9/8}TiS_3$ is presented in Figure 5.2. From the illustration it can be seen that the four-dimensional model differ slightly from the three-dimensinal in the positioning of the barium and selenium atoms.

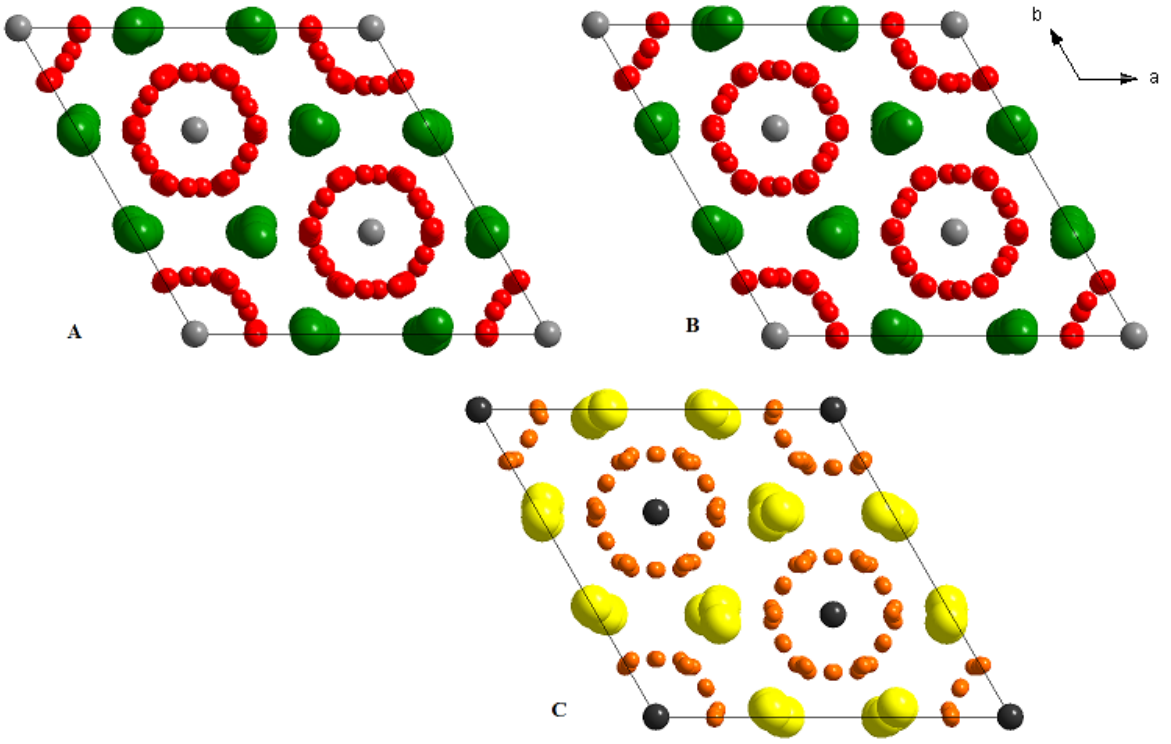

Figure 5.2. Comparison of $Ba_{15}Zr_{14}Se_{42}$ from the three-dimensional model (A) with the four-dimensional model (B) and $Sr_{9/8}TiS_3$ (C), along the c-axis. The atoms correspond to barium (green), selenium (red), strontium (yellow), sulfur (orange), titanium (dark grey) and zirconium (light grey).

The model includes four different atoms to describe the structure of $Ba_{15}Zr_{14}Se_{42}$; Ba1, Zr1, Se1 and Se2. All the atomic positions in the structure can be described by symmetry

operations of these four atoms. This shows the simplification compared to the three-dimensional model which includes a total of 18 atoms to describe the structure [1]. The reason for the decrease of atoms needed is that the translational symmetry is recovered in four dimensions. The unusually long *c*-axis of $Ba_{15}Zr_{14}Se_{42}$ arises from the mismatching of the atomic positions in three dimensions which gives rise to the loss of translational symmetry along the *c*-axis. Thus, more atoms are needed to describe all the atomic positions in the unit cell. This problem disappears in four dimensions where an extra vector (*q*) is added to describe how the subunits relate to each other, in this case $[ZrSe_{6/2}]$-units and Ba-atoms. Thus the translational symmetry obtained along the *q*-vector give rise to a simpler model. The atomic positions in three dimensions (commensurate case) that is obtained from the model are presented in Table 5.3. These atomic positions are similar to those reported for $Sr_{9/8}TiS_3$ [2].

Table 5.3. Fractional atomic coordinates for the commensurate case of $Ba_{15}Zr_{14}Se_{42}$ in three-dimensions.

Atom	*x*	*y*	*z*
Ba1	0.339730	0	0.25000
Zr1	0	0	0
Se1	0.169092	0.169092	0.50000
Se2	0.080671	0.183987	0.641728

5.2 Four-dimensional Modeling of $Sr_{21}Ti_{19}Se_{57}$

A model was also made with starting point in the $Sr_{21}Ti_{19}Se_{57}$ structure. The indexation of *l* and *m* were made by hand from the known repeat of the different subunits. This unit cell is bigger than the barium-case and the repeats were found to be 38 for the $[TiSe_{6/2}]$-units and 21 for the strontium atoms. The handmade indexation is presented in Appendix D. The correlations were a bit more complicated for this structure and due to the larger unit cell, more reflections had to be generated from the three-dimensional data. The four-dimensional crystal parameters used are summarized in Table 5.4.

Table 5.4. Crystallographic data for $Sr_{21}Ti_{19}Se_{57}$.

Crystal system	Trigonal
Space group	R-3m(00γ)0s
a* = *b	11.9517 Å
c	3.1026 Å
α = β	90 °
γ	120 °

JANA2006 had problem reading the amount of generated *hklm*-reflections and the model could not be made from only these. Since $Ba_{15}Zr_{14}Se_{42}$ is isostructural to $Sr_{21}Ti_{19}Se_{57}$ the atomic data obtained in the first model (positions of atoms and occupation etc.) could be transferred and refined with the new reflection data. This was done by copying the m40 file for the first model and insert it in the strontium case and change the atoms to the correct ones. There were however still problems with too much reflection data that were locking the positions of the atoms (explained previously).

The model was modified to only consider up to fifth order satellites to make it more realistic and this lowered the R-value of the model significantly. The overall R-value for the structure was refined down to 4.67% with a GoF of 1.71. The R-values for the main reflections, satellites and each subunit are presented in Table 5.5.

Table 5.5. Final residual factors for the four-dimensional model of $Sr_{21}Ti_{19}Se_{57}$.

	R(obs) [%]	**wR(obs) [%]**	**Observed reflections/All**
Main reflections	1.75	3.04	600/1105
1 order satellites	2.69	4.08	751/1500
2 order satellites	3.96	5.37	452/909
3 order satellites	5.72	6.92	262/619
4 order satellites	7.07	9.37	161/389
Structure	2.99	4.67	2296/4760
Sub1 [Sr]	1.66	2.72	244/400
Sub2 [$TiSe_{6/2}$]	2.00	3.55	301/631
Common	1.21	1.81	55/74

The atomic positions for the commensurate case in three dimensions that is obtained from the model are presented in Table 5.6. Just as for the $Ba_{15}Zr_{14}Se_{42}$ model four atoms are needed to describe the structure compared to the 48 needed in the three-dimensional case [1]. The overall discussion and reasoning regarding this model is the same as for the $Ba_{15}Zr_{14}Se_{42}$ model. A comparison of the three-dimensional model, the four-dimensional model made in this study and $Sr_{9/8}TiS_3$ is presented in Figure 5.3. It is also here possible to see slight variations in the position of the strontium and selenium atoms between the four-dimensional and three-dimensional model.

Table 5.6. Fractional atomic coordinates for the commensurate case of $Sr_{21}Ti_{19}Se_{57}$ in three-dimensions.

Atom	*x*	*y*	*z*
Sr1	0.344418	0	0.25000
Ti1	0	0	0
Se1	0.194505	0.194505	0.50000
Se2	0.102127	0.178514	0.474140

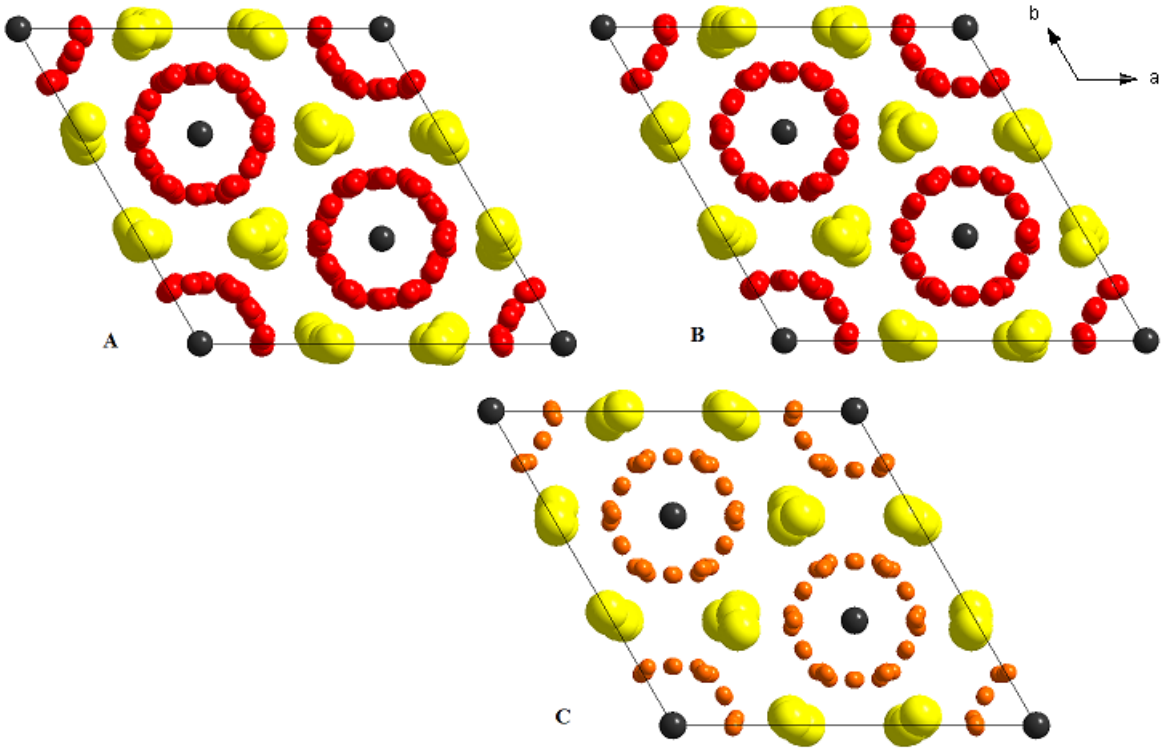

Figure 5.3. Comparison of $Sr_{21}Ti_{19}Se_{57}$ from the three-dimensional model (A) with the four-dimensional model (B) and $Sr_{9/8}TiS_3$ (C), along the c-axis. The atoms correspond to selenium (red), strontium (yellow), sulfur (orange) and titanium (dark grey).

5.3 Results from synthesis

5.3.1 Experimental difficulties

The synthesis of the two compounds proved to be more difficult than could be deduced from the original report [1]. Since no ampoule material was stated various were tried in this study but without any luck. The silica tubes were not strong enough to withstand the vapor pressure of selenium. The attempts to synthesize in metallic tubes resulted in the loss of selenium due to reaction with the tube. Only in one of the samples, crystals including the three wanted elements could be found but not in the right proportions. It is clear that the synthesis is not as easy as first assumed and another approach with different starting materials would definitely be worth considering.

5.3.2 $Ba_{21}Zr_{12}Se_{45}$

In the sample from synthesis B1, about a dozen small, black and rod-shaped crystals could be found. Pre-analysis was made using single crystal diffraction it was found that they seemed to have a variety of unit cells. However, only two of them had a quality high enough for continued characterization. One ternary compound including the wanted elements could be identified. The compound, $Ba_{21}Zr_{12}Se_{45}$, has the same selenium ratio as the desired compound but differs in the barium-zirconium ratio. Compared to $Ba_{15}Zr_{14}Se_{42}$, this compound has nearly twice as much barium compared to zirconium. The new compound crystalizes in the trigonal space group R-3m with the cell parameters a = 21.9115(19) Å, c = 16.7445(9) Å and the structure was refined down to an R-value of 7.60%. A more specific description of the unit cell with atomic position and such can be found in Appendix E. Figure 5.4 shows an illustration of the compound.

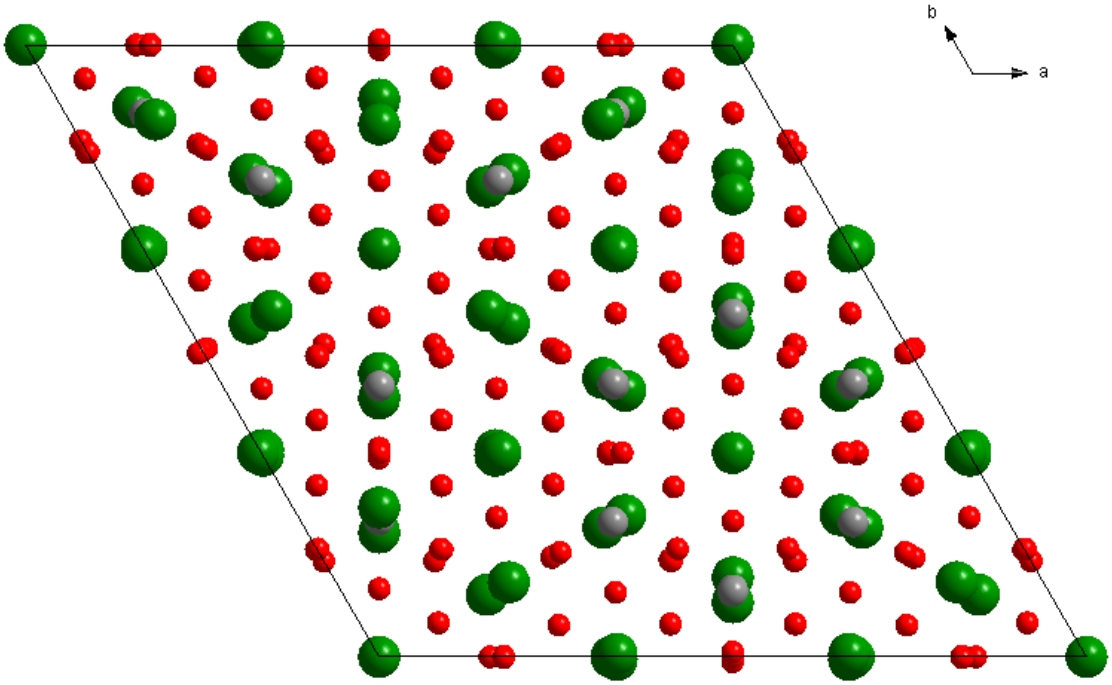

Figure 5.4. The unit cell of $Ba_{21}Zr_{12}Se_{45}$, viewed along the c-axis. Barium (green), selenium (red) and zirconium (light grey).

The structure is somewhat similar to that of $Ba_{15}Zr_{14}Se_{42}$ as well. It consists out of octahedral units of zirconium and selenium with barium atoms in the cavities between. The octahedra are linked together in pairs through face sharing and connected to other octahedral pairs through corner sharing. This becomes more clear in Figure 5.5 where the octahedra are displayed and the barium atoms hidden. The structure does not form the same chain-like structure as previously known case due to the lack of mismatching in the translational symmetry. This makes the unit cell smaller. Figure 5.6 shows the unit cell with both the coordination octahedra displayed and the barium atoms shown. As can be seen, the barium atoms are located in the cavities between the octahedra. There are however more than one position, the ones surrounded by six octahedra and the ones in-between two corner-sharing octahedra. The barium positions 1-3 corresponds to the barium atoms that are surrounded by six octahedrons whereas the positions 4-5 are the ones between the corner-sharing octahedra.

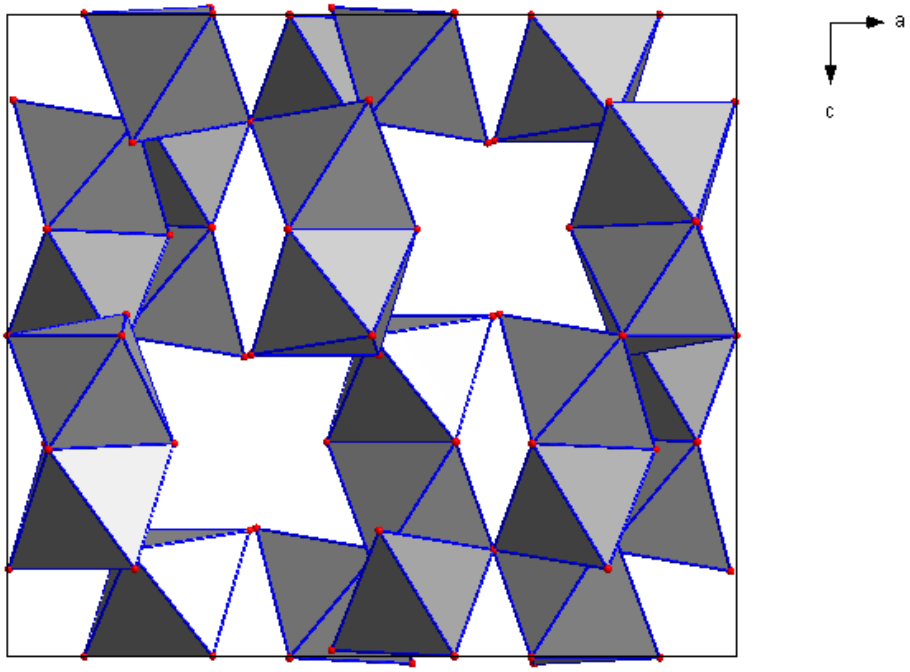

Figure 5.5. The unit cell of $Ba_{21}Zr_{12}Se_{45}$ viewed along the b-axis. The coordination octahedra are illustrated with zirconium (light grey) at the center and selenium (red) at the vertex positions. Both the vertex-sharing and the face-sharing of the octahedra can be seen.

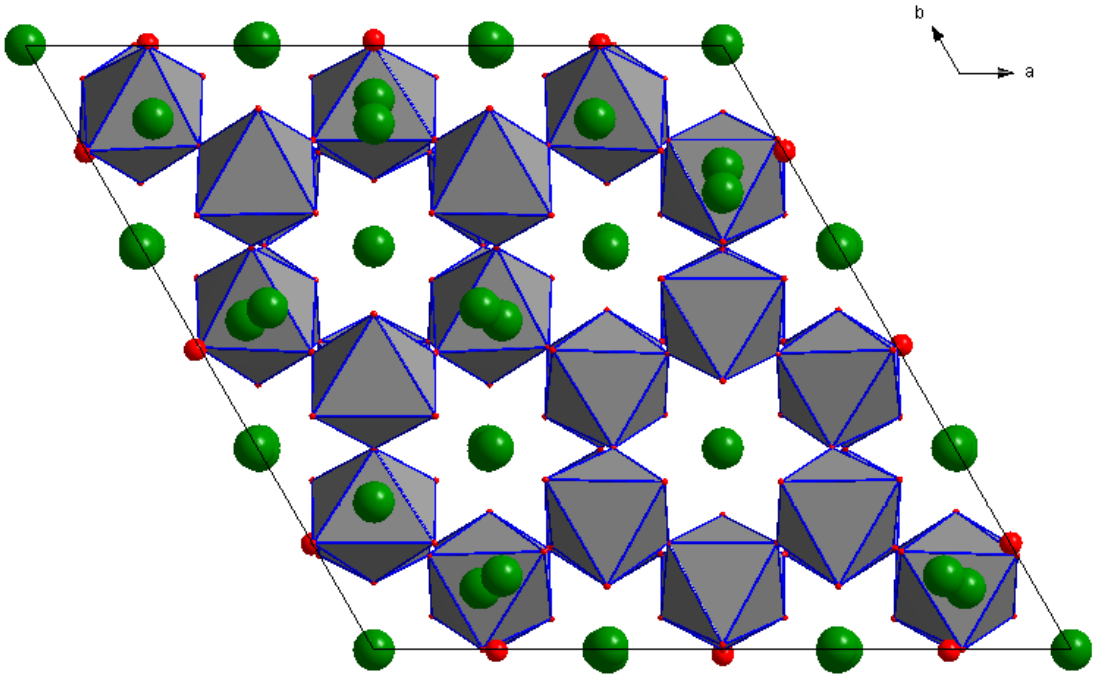

Figure 5.6. The unit cell of $Ba_{21}Zr_{12}Se_{45}$ viewed along the c-axis. The coordination octahedra are illustrated with zirconium (light grey) at the center and selenium (red) at the corner positions. The corner-sharing of the octahedra can be seen and the positions of the barium atoms (green).

5.3.3 $BaSe_2O_6$

The other new compound found is an oxide with a probable composition of $BaSe_2O_6$. It has a triclinic structure with cell parameters a = 6.074 Å, b = 8.3001 Å and c = 9.8789 Å with α = 75.602°, β = 73.677° and γ = 71.451°. The structure was refined down to an R-value of 3.21%. A more specific description of the unit cell with atomic position and such can be found in Appendix F.

It only differs 6 electrons in the atoms of selenium and zirconium which makes their electron densities similar. A refinement was made with zirconium instead of selenium but the R-value became slightly higher (3.73%).

The findings of this compound shows that the samples had not been sufficiently protected from oxygen. Almost all the starting materials are sensitive to water or air. Due to the available equipment it was not possible to work exclusively in an oxygen-free environment due to transportations between the different apparatus. The exposure was however kept to a minimal. Another possibility is that some of the starting materials was partly oxidized to start with.

6. Conclusions

The synthesis of the two ternary selenium compounds turned out to be harder than could be interpreted from the original article [1]. In fact, neither of the two stated compounds could be synthesized in this study. The four-dimensional model is thus made from the three-dimensional data published in the original article [1].

The refined models of $Ba_{15}Zr_{14}Se_{42}$ and $Sr_{21}Ti_{19}Se_{57}$ show great similarities with the four-dimensional model made by Gourdon et.al for $Sr_{9/8}TiS_3$ [2]. Both structures are modeled with four atoms. The barium and strontium atoms along with the selenium atoms have occupancies described by harmonic functions. The models was refined down to an R-value of 4.98% and 4.67% for $Ba_{15}Zr_{14}Se_{42}$ and $Sr_{21}Ti_{19}Se_{57}$, respectively. These values give decent models but which are still refinable. Overall, there is a strong indication that the sulfur cases are isostructural to the selenium cases.

One new, previously unknown compound $Ba_{21}Zr_{12}Se_{45}$ was found during the synthesis. It crystalizes in the trigonal space group R-3m and has cell parameters of a = 21.9115(19) Å and c = 16.7445(9) Å. It does not show the same columnar composite behavior as the previously known structure. Thus a smaller unit cell is observed and the four-dimensional model made, is not applicable to this compound. An oxide with a probable composition of $BaSe_2O_6$ was also found. It has a triclinic structure with cell parameters a = 6.074 Å, b = 8.3001 Å, c = 9.8789 Å, $\alpha = 75.602°$, $\beta = 73.677°$ and $\gamma = 71.451°$.

6.1 Scientific, Social and Ethical Aspects

This report does not have a direct applicational goal but strives towards a greater understanding of how atoms interact with each other and how this effect the structure of a crystal and thus the material. The requirements for new and better materials are constantly increasing. Environmentally unfriendly materials are being phased out of use and materials with equal or better properties needs to be found. To be able to find and construct equivalent materials it is important to know the reason behind the properties. In the end it is the knowledge of the interactions of the atoms and their crystal structures that determines the properties of a crystalline material which makes it important to understand. Problems arising with the search of new materials is the possible lack of legislation for new compounds. The health effects and environmental impact of new materials can take years to conclude. One of the biggest issue might be in trying to explain the relevance of this type of research. It is hard over all for people to understand the necessity of this type of research. It is easier to understand if there is a direct application that follows.

Research is important, the more we learn about atomic interactions the more we can use that knowledge to our advantage. Even if this particular project did not contribute to any significant findings, it is a contribution in which I have learnt a lot. Not only about crystallography, but also about laboratory work and independent planning. In the end it has served its purpose as the final part of this education where I got to experience the problems and difficulties that a materials engineer might encounter.

7. Future Work

Future work would be to continue in trying to solve the experimental difficulties and synthesize the two ternary selenium compounds, $Sr_{21}Ti_{19}Se_{57}$ and $Ba_{15}Zr_{14}Se_{42}$ and then use the obtained data to make a more refined model of the structure. The first approach would be continued synthesis in platina tubes enclosed in niobium tubes. Even though the right compound was not found, a compound including the right elements was obtained which shows that the synthesis works. Another approach would be to use other starting materials than the ones used in this study. One approach could be to start synthesizing in similar manner as Gourdon et.al did for the sulfur compound[2].

The four-dimensional models are not perfect and continued work with these to lower the R-values further should be carried out. Best case scenario would of course be to make the model from real data sets where all the intensities and reflections correspond to the actual crystal.

The two ternary systems are not that well explored and from the findings of $Ba_{21}Zr_{12}Se_{45}$ it is clear that there might be more interesting compounds to be found. Further work regarding this new compound would be trying to refine it further to lower the residual factors. This would include doing absorption calculations for the crystal and also trying to find a cleaner version of the crystal to obtain better results.

8. Reference list

[1] L. Tranchitella, J. Fettinger, P. Dorhout, P. Van Calcar, and B. Eichhorn, "Commensurate Columnar Composite Compounds: Synthesis and Structure of Ba15Zr14Se42 and Sr21Ti19Se57," *J. Am. Chem. Soc.*, vol. 120, no. 30, pp. 7639–7640, 1998.

[2] O. Gourdon, V. Petricek, and M. Evain, "A new structure type in the hexagonal peroskite family; structure determination of the modulated misfit compound Sr9/8TiS3," *Acta Crystallogr. B*, vol. 56, pp. 409–418, 2000.

[3] M. Onoda and M. Saeki, "Rietveld Analysis of an Incommensurate Composite Crystal with a Nominal Composition Sr1.19TiS3," *Jpn. J. Appl. Phys.*, vol. 32, pp. 752–753, 1993.

[4] M. Onoda, M. Saeki, A. Yamamoto, and K. Kato, "Structure Refinement of the Incommensurate Composite Crystal Sr1.145TiS3 Through the Rietveld Analysis Process," *Acta Crystallogr. B*, vol. 49, pp. 929–936, 1993.

[5] M. Saeki and M. Onoda, "Preparation of a Chain-type Composite Crystal, BaxTiS3 (x = 1.00-1.05)," *J. Solid State Chem.*, vol. 112, pp. 65–69, 1994.

[6] M. Saeki and M. Onoda, "Preparation of a new Strontium Titanium Sulfide SrxTiS3 (x = 1.05 - 1.22) with Infinitely Adaptive Structures," *J. Solid State Chem.*, vol. 102, pp. 100–105, 1993.

[7] J. Sun, S. Lee, and J. Lin, "Four-dimensional space groups for pedestrians: Composite structures," *Chem. - An Asian J.*, vol. 2, no. 10, pp. 1204–1229, 2007.

[8] L. Smart and E. Moore, *Solid State Chemistry - An Introduction*, Fourth Edi. 2012.

[9] C. Giacovazzo, H. L. Monaco, D. Viterbo, F. Scordari, G. Gilli, G. Zanotti, and M. Catti, *Fundamentals of Crystallography*. Oxford University Press, 1992.

[10] P. Bak, "Commensurate phases , incommensurate phases and the devil ' s staircase," *Rep. Prog. Phys.*, vol. 45, no. July 1981, p. 587, 1982.

[11] H. Hahn and U. Mutschke, "Versuche zur Darstellung von Thioperowskiten," *Z. Anorg. Allg. Chem.*, no. 288, pp. 269–278, 1956.

[12] A. West, *Basic Solid State Chemistry*. 1984.

Appendix A – Crystal Structures

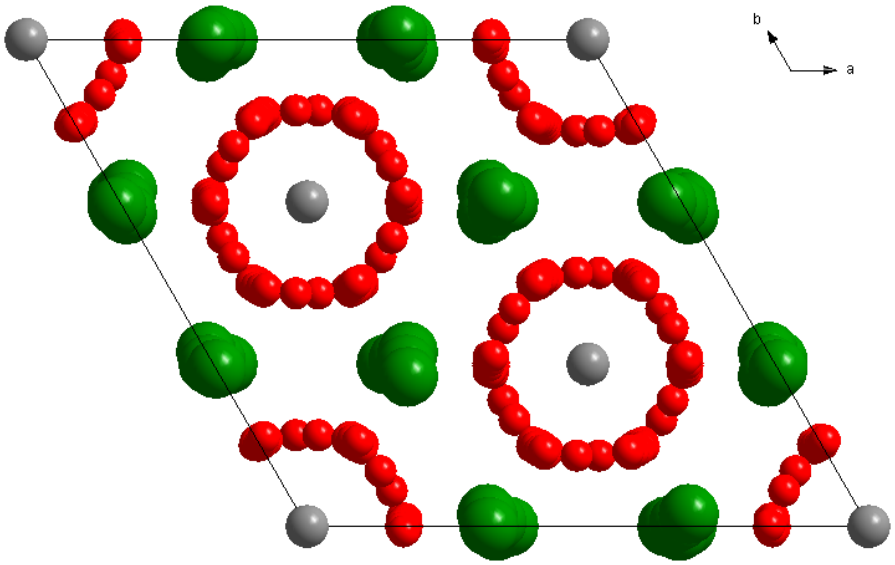

Figure A1. The crystal structure of $Ba_{15}Zr_{14}Se_{42}$ [1] *viewed along the c-axis. The atoms correspond to barium (green), zirconium (light grey) and selenium (red).*

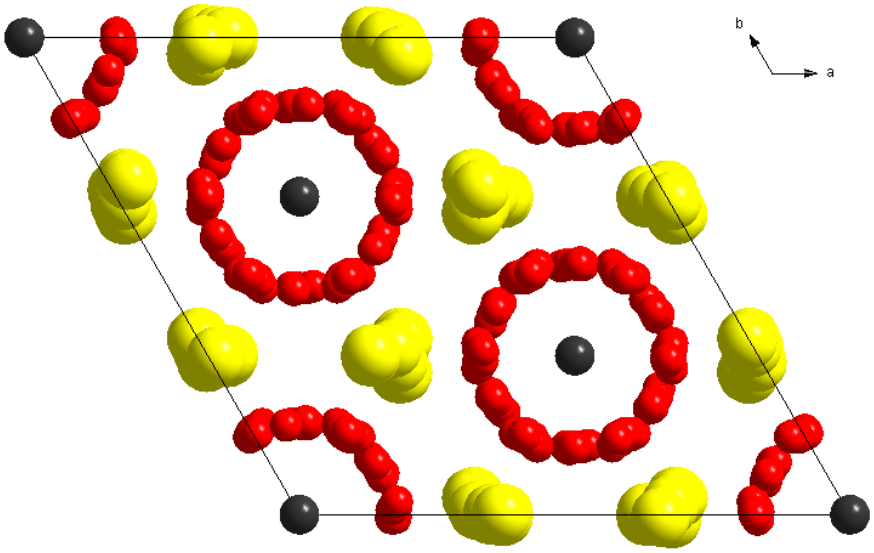

Figure A2. The crystal structure of $Sr_{21}Ti_{19}Se_{57}$ [1] *viewed along the c-axis. The atoms correspond to strontium (yellow), titanium (dark grey) and selenium (red).*

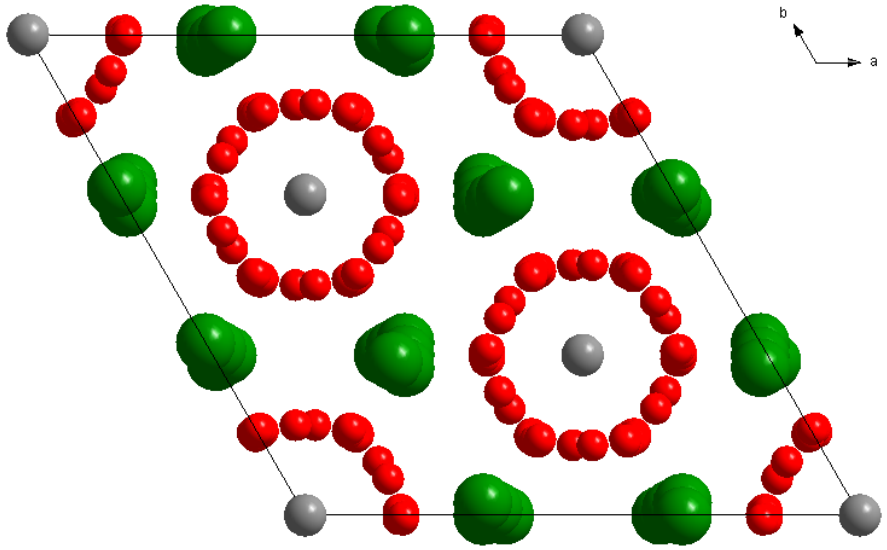

Figure A3. The crystal structure of $Ba_{15}Zr_{14}Se_{42}$ generated from the four-dimensional model, viewed along the c-axis. The atoms correspond to barium (green), zirconium (light grey) and selenium (red).

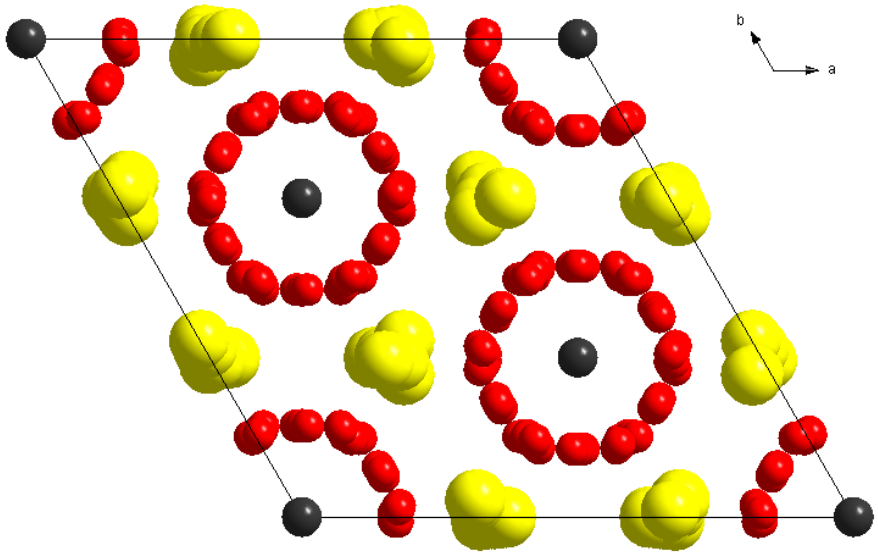

Figure A4. The crystal structure of $Sr_{21}Ti_{19}Se_{57}$ generated from the four-dimensional model, viewed along the c-axis. The atoms correspond to strontium (yellow), titanium (dark grey) and selenium (red).

Appendix B – Sample Preparation

Table B1. Summarization of the sample preparation of $Sr_{21}Ti_{19}Se_{57}$. The molar amounts of raw material are presented along with the weight percent of flux used in each synthesis. It is also stated how the synthesis was made along with temperatures and annealing times. Sample S6 was first annealed at 1050 °C and then at 600 °C for 142 and 24 h, respectively.

Sample	$\mathbf{n_{SrSe}}$ [**mol**]	$\mathbf{n_{Ti}}$ [**mol**]	$\mathbf{n_{Se}}$ [**mol**]	$\mathbf{SrCl_2}$ [**wt**%]	Synthesis	Heat treatment [°C]	Time [h]
S1	0.00269	0.00268	0.00540	10.3	Evacuated quartz tube	1050	N.A
S2	0.00269	0.00267	0.00536	10.5	Evacuated quartz tube	1050	N.A
S3	0.00201	0.00201	0.00401	10.3	Alumina crucible in evacuated niobium tube	1000	88
S4	0.00202	0.00202	0.00403	10.6	Evacuated quartz tube	950	87
S5	0.00202	0.00202	0.00403	12.5	Alumina crucible in evacuated niobium tube	1100	191
S6	0.00202	0.00198	0.00399	12.8	Evacuated quartz tube in niobium tube with water for counter pressure	1050	121
S7	0.00137	0.00138	0.00273	21.0	Alumina crucible in evacuated niobium tube	$1050 \rightarrow 600$	142 + 24

Table B2. Summarization of the sample preparation of BaSe. BaSe-3 was annealed in 600 °C for 48 h and then the temperature was raised to 712 for 5 h.

Sample	$\mathbf{n_{Ba}}$ [**mol**]	$\mathbf{n_{Se}}$ [**mol**]	Synthesis	Heat treatment [°C]	Time [h]
BaSe-1	0.00330	0.00333	Evacuated quartz tube	650	N.A
BaSe-2	0.00357	0.00358	Evacuated quartz tube	500	N.A
BaSe-3	0.00457	0.00453	Platinum tube in evacuated stainless steel tube	$600 \rightarrow 712$	48 + 5

Table B3. Summarization of the sample preparation of $Ba_{15}Zr_{14}Se_{42}$. Sample B2 was first annealed at 1050 °C and then at 600 °C for 109 h and 24 h, respectively.

Sample	$\mathbf{n_{BaSe}}$ [**mol**]	$\mathbf{n_{Zr}}$ [**mol**]	$\mathbf{n_{Se}}$ [**mol**]	$\mathbf{BaCl_2}$ [**wt%**]	Synthesis	Heat treatment [°C]	Time [h]
B1	0.00157	0.00158	0.00317	39.6	Platinum tube in evacuated niobium tube	1050	137
B2	0.00164	0.00158	0.00326	39.0	Platinum tube in evacuated niobium tube	$1050 \rightarrow 600$	109 + 24

Appendix C – Powder Diffraction data BaSe

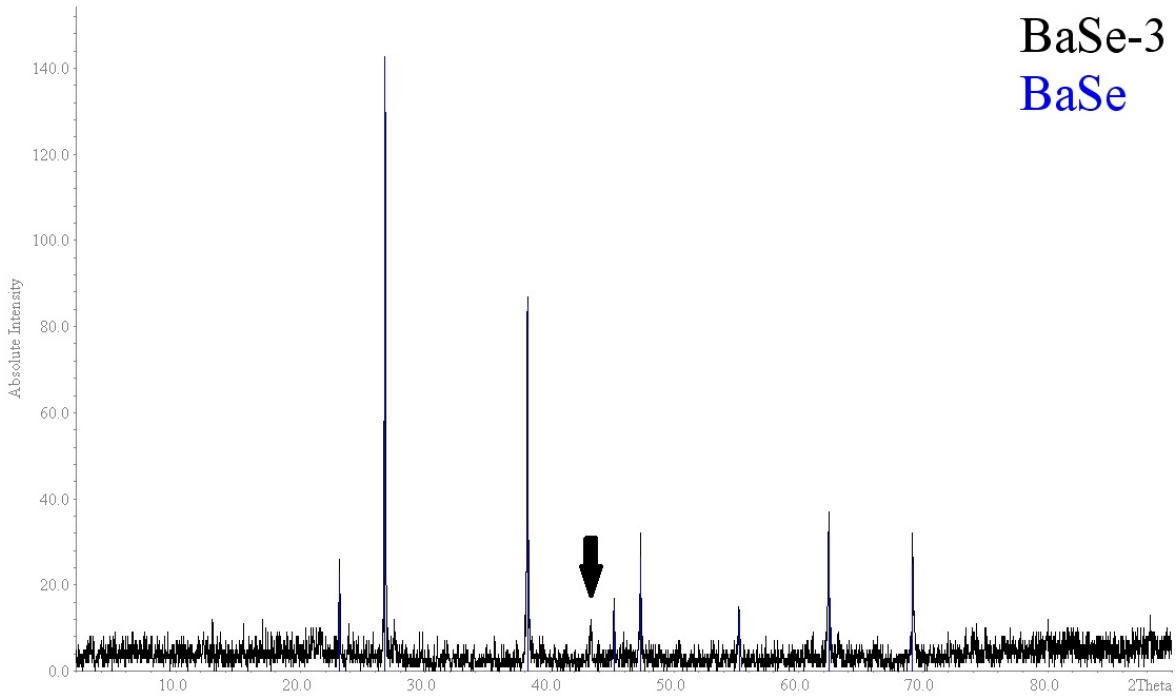

Figure C1. Powder diffraction data from the synthesis of BaSe (BaSe-3). The peaks that correspond to the wanted compound, BaSe, are marked with blue. The black arrow marks the only significant peak that does not belong to the wanted compound.

Appendix D – Indexation

Table D1. Indexation of the l and m parameters for $Ba_{15}Zr_{14}Se_{42}$.

Main reflections	Satellites
1, 0	
	-6, 13
	2, -2
	-5, 11
	3, -4
	-4, 9
	4, -6
	-3, 7
	5, -8
	-2, 5
	6, -10
	-1, 3
	7, -12
	0, 1
	-7, 14
	1, -1
	-6, 12
	2, -3
	-5, 10
	3, -5
	-4, 8
	4, -7
	-3, 6
	5, -9
	-2, 4
	6, -11
	-1, 2
	7, -13
0, 0	
	-7, 13
	1, -2
	-6, 11
	2, -4
	-5, 9
	3, -6
	-4, 7
	4, -8
	-3, 5
	5, -10
	-2, 3
	6, -12
	-1, 1
	7, -14
	0, -1
	-7, 12
	1, -3
	-6, 10
	2, -5
	-5, 8
	3, -7
	-4, 6
	4, -9
	-3, 4
	5, -11
	-2, 2
	6, -13
-1, 0	

Table D2. Indexation of the l and m parameters for $Sr_{21}Ti_{19}Se_{57}$.

Main reflections	Satellites
1, 0	
	-4, 9
	-9, 18
	7, -11
	2, -2
	-3, 7
	-8, 16
	8, 13
	3, -4
	-2, 5
	-7, 14
	9, -15
	4, -6
	-1, 3
	-6, 12
	10, -17
	5, -8
	0, 1
	-5, 10
	-10, 19
	6, -10
	1, -1
	-4, 8
	-9, 17
	7, -12
	2, -3
	-3, 6
	-8, 15
	8, -14
	3, -5
	-2, 4
	-7, 13
	9, -16
	4, -7
	-1, 2
	-6, 11
	10, -18
	5, -9
0, 0	
	-5, 9
	-10, 18
	6, -11
	1, -2
	-4, 7
	-9, 16
	7, -13
	2, -4
	-3, 5
	-8, 14
	8, -15
	3, -6
	-2, 3
	-7, 12
	9, -17
	4, -8
	-1, 1
	-6, 10
	10, -19
	5, -10
	0, -1
	-5, 8
	-10, 17
	6, -12
	1, -3
	-4, 6
	-9, 15
	7, -14
	2, -5
	-3, 4
	-8, 13
	8, -16
	3, -7
	-2, 2
	-7, 11
	9, -18
	4, -9
-1, 0	

Appendix E – Cell Parameters and Atomic Positions of $Ba_{21}Zr_{12}Se_4$

Table E1. Cell parameters for the compound $Ba_{21}Zr_{12}Se_4$.

Space group	R-3m (166) trigonal
a* = *b	21.9115(19) Å
c	16.7445(9) Å
α = β	90 °
γ	120 °
c/a	0.7642
V	6962.21(90) $Å^3$
Z	3

Table E2. Atomic positions for the different atoms included in the compound $Ba_{21}Zr_{12}Se_4$.

Atom	*x*	*y*	*z*
Ba1	0	0	0.16575
Ba2	1/3	2/3	1/6
Ba3	1/3	-0.00459	1/6
Ba4	0.12209	0.24418	0.00886
Ba5	0.56504	0.13008	0.01591
Zr1	0.22004	0.44008	0.09454
Zr2	0.44274	0.22137	0.10785
Se1	0.38680	0.10529	0.00113
Se2	0.49592	0.50408	0.13351
Se3	0.55526	0.27763	0.0104
Se4	0.17650	0.00148	0.13692
Se5	0.17675	0.51008	1/6
Se6	1/3	1/6	1/6

Appendix F – Cell Parameters and Atomic Positions of $BaSe_2O_6$

Table F1. Cell parameters for the compound $BaSe_2O_6$.

Space group	P-1(2) Triclinic
a	6.074(5) Å
b	8.3001(7) Å
c	9.8789(8) Å
α	75.602(7) °
β	73.677(7) °
γ	71.451(7) °
c/a	1.6264
V	446.14(7) $Å^3$
Z	2

Table F2. Atomic positions for the different atoms included in the compound $BaSe_2O_6$.

Atom	*x*	*y*	*z*
Ba1	0.84068	0.79188	0.45440
Se1	0.39302	0.18577	0.04015
Se2	0.30459	0.48640	0.01203
O1	0.59272	0.66632	0.33624
O2	1.22555	0.94718	0.36983
O3	0.75577	0.47561	0.63299
O4	0.99375	0.86386	0.15182
O5	0.39733	0.86375	0.65563
O6	1.12148	0.65090	0.66302